Current Applied Physics 11 (2011) S238–S241

Contents lists available at ScienceDirect

Current Applied Physics

journal homepage: www.elsevier.com/locate/cap

High-performance $GdBaCo_2O_{5+\delta}$–$Ce_{0.9}Gd_{0.1}O_{1.95}$ composite cathode for solid oxide fuel cells

Seung Jun Lee, Dong Seok Kim, Do Kyung Kim*

Department of Materials Science and Engineering, Korea Advanced Institute of Science and Technology (KAIST), 335 Gwahak-ro, Yuseong-gu, Daejeon 305-701, Republic of Korea

ARTICLE INFO

Article history:
Received 30 August 2010
Accepted 1 November 2010
Available online 5 November 2010

Keywords:
Composite cathode
Double-perovskite
Electrochemical performance
Solid oxide fuel cells

ABSTRACT

$GdBaCo_2O_{5+\delta}$ (GBCO)–$Ce_{0.9}Gd_{0.1}O_{1.95}$ (CGO) composites with various CGO contents (0–40 wt.%) have been investigated for potential cathode materials for intermediate temperature solid oxide fuel cells (IT-SOFCs). The effect of CGO incorporation on the thermal expansion coefficient (TEC), electrochemical performance and microstructure of the GBCO–CGO composite cathodes are investigated. The thermal expansion behavior shows that the TEC values of GBCO cathode decrease with CGO addition. The TEC of 30 wt.% CGO–70 wt.% GBCO (CG30) cathode shows 14.7×10^{-6} °C^{-1} up to 900 °C, which is lower value than pristine GBCO (20.0×10^{-6} °C^{-1}). In addition, the addition of CGO to GBCO cathode improves remarkably the electrochemical performance. The composite cathode of 30 wt.% CGO–70 wt.% GBCO (CG30) coated on $Ce_{0.9}Gd_{0.1}O_{1.95}$ electrolyte shows the lowest polarization resistance (0.029 Ω cm^2 at 700 °C). An electrolyte-supported (300 μm thick) single-cell configuration of CG30/CGO/Ni-CGO attains a maximum power density of 340 and 525 mW cm^{-2} at 650 and 700 °C, respectively. The results indicate that 30 wt.% CGO–70 wt.% GBCO cathode is a promising cathode material for IT-SOFCs.

1. Introduction

In recent years, solid oxide fuel cells (SOFCs) have attracted much interest as one of the promising power generation technologies because of their advantages in high working efficiency, low pollution and fuel flexibility [1–5]. Lowering the operation temperature of SOFCs to intermediate temperature regions (600–800 °C) can not only extend the range of materials selection, significantly reduce the cost of production, but also improve the stability and reliability for the SOFCs system. In the intermediate temperature region, however, it is generally established that the cathode becomes one of the major obstacle in determining the overall cell performance because the polarization resistance increases rapidly as the temperatures decreases [4–6]. Thus, the development of electrodes with high performance related to the interfacial resistance is essential for IT-SOFCs.

Recent studies on double-perovskite structure have reported electrochemical properties of a new type of mixed ionic electronic conductor (MIEC) oxides, i.e. cation ordered $LnBaCo_2O_{5+\delta}$ (Ln = La, Pr, Sm, Gd, Y) as potential cathode materials for IT-SOFCs [7–11]. In particular, $GdBaCo_2O_{5+\delta}$ (GBCO) has been reported to exhibit ionic conductivity due to the oxygen vacancies that are mainly located in the rare-earth planes and high electronic conductivity [9,10]. However, cobalt-based cathode materials have high thermal expansion coefficients (TECs) that are not compatible with those of intermediate temperature electrolytes [6,9]. The thermal expansion mismatch can cause delamination or cracking at the interface of cathode and electrolyte, thus results in its thermal cycling and long-term thermal stability performance [6,12]. Therefore, it is important to improve the thermal expansion mismatch between the cathode and the electrolyte. One of the ways to reduce the TEC is change in the Ln ion radius, i.e. TEC decrease with decreasing size of Ln^{3+} ions from Ln = La to Gd [6]. Another effective way to reduce the TEC is incorporation of electrolyte materials to cathode to form a composite cathode [4,12,13]. In addition, the composite can also expand the electrochemically active triple phase boundaries (TBP), at which the oxygen reduction reaction occurs and enhance electrochemical performance [2,13–15]. With aim of reducing mismatch in TEC between the electrolyte and cathode materials and improving electrochemical performance, we investigate the thermal expansion behavior and electrochemical performance of GBCO–CGO composites cathodes.

2. Experiment

Double-perovskite oxides of $GdBaCo_2O_{5+\delta}$ (GBCO) was prepared by a citrate combustion method using analytical grade Gd $(NO_3)_3.6H_2O$ (>99.9%), $Ba(NO_3)_2$ (99+%), $Co(NO_3)_2.2.5H_2O$ (98+%)

* Corresponding author. Tel.: +82 42 350 4118; fax: +82 42 350 3310.
E-mail address: dkkim@kaist.ac.kr (D.K. Kim).

1567-1739/$ – see front matter © 2010 Elsevier B.V. All rights reserved.
doi:10.1016/j.cap.2010.11.010

and citric acid (99%). The citric acid combustion method had been described in detail in our previous work [2,9].

The stoichiometric amount of $Ce(NO_3)_3.6H_2O$ (99.9%), $Gd(NO_3)_3.6H_2O$ (99.9%) were dissolved in 50 ml of ethanol to form calculated x wt.% $Ce_{0.9}Gd_{0.1}O_{1.95}$ in composite. To the above clear solution, (100-x) wt.% of calcined GBCO powder was dispersed under sonication for 2 h. The $(C_2H_5)_2NH$ (diethylamine, 99.9%) precipitant was used to precipitate the CGO in the presence of GBCO to form the composite. Thus, obtained composite powders were calcined at 900 °C for 10 h. The GBCO and CGO composites had a composition varying from 0 to 40 wt.%, and the designations of these cathodes are summarized in Table 1.

The phases of the synthesized powders were characterized with an X-ray diffractometer (XRD) (Rigaku, D/MAX-RB X-ray diffractometer) equipped with Cu–Kα radiation ($\lambda = 0.15406$ nm). The TEC for each rectangular-shape pellets sintered at 1000 °C for 2 h was measured using a dilatometer (NETZSCH DIL402C) from 30 to 900 °C. The microstructure of the cell interface between cathode and CGO electrolyte was examined with a scanning electron microscope (FE-SEM Philips XL30 FEG).

Symmetrical cells, with a CGO–GBCO/CGO/CGO–CBCO configuration, were used for the area specific resistances (ASRs) measurements. The cathode was screen-printed on the dense CGO electrolyte pellets and sintered at 950 °C for 2 h in air to form an effective cathode surface area of 0.385 cm^2. Pt paste (ESL) was applied to the edge of the same side of the working electrode on the electrolyte to act as the reference electrode. ASRs were measured via 3-probe AC impedance spectroscopy (Solartron 1260 impedance/Gain-phase analyzer) as a function of temperature (500–800 °C) in flowing air. The sweeping frequency range was 10^6–10^{-2} Hz with signal amplitude of 10 mV.

Single cell was fabricated by electrolyte-supported technique with 300 μm CGO as the electrolyte, CG30 as the cathode, and NiO-CGO (in a weight ratio of 65:35) as the anode were fabricated using screen-printing method. A Source meter (Keithley 2400) was used to measure *I-V* polarization under flowing humidified H_2 (~3% H_2O) as a fuel, and air as an oxidant.

3. Result and discussions

Fig. 1 shows the XRD patterns of GBCO (CG0) and CG30 cathode calcined at 900 °C for 10 h. The XRD pattern of GBCO is represented by a single-phase, high crystalline double-perovskite structure. All the diffraction peaks can be indexed based on the JCPDS #53-0135 with an orthorhombic structure, space group *Pmmm*. The unit cell parameters for GBCO are $a = 3.875$ Å, $b = 3.911$ Å and $c = 7.531$ Å, and the cell volume is 114.133 $Å^3$, which are in good agreement with literature results [7–10]. After the GBCO–30 wt.% CGO mixture has been calcined at 900 °C for 10 h, the GBGO and CGO still retain their own structures without any secondary phase. The XRD investigations confirm that GBCO and CGO have a good chemical compatibility when the operating temperature is below 900 °C.

Fig. 2 shows the thermal expansion curves for different wt.% CG composite cathodes and the table in inset shows the

Table 1
Chemical compositions and their designations.

Chemical composition	Designation
$GdBaCo_2O_{5+\delta}$	GBCO (CGO)
$Ce_{0.9}Gd_{0.1}O_{1.95}$	CGO
10 wt.% CGO and 90 wt.% GBCO	CG10
20 wt.% CGO and 80 wt.% GBCO	CG20
30 wt.% CGO and 70 wt.% GBCO	CG30
40 wt.% CGO and 60 wt.% GBCO	CG40

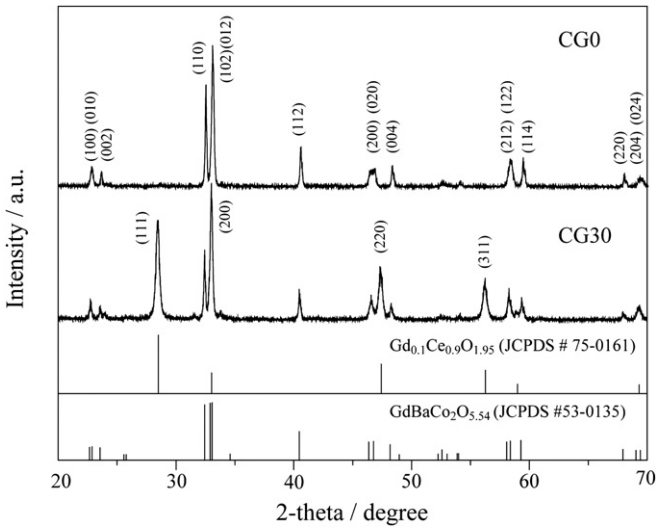

Fig. 1. XRD patterns of the $GdBaCo_2O_{5+\delta}$ (CG0) and CG30 powers calcined at 900 °C for 10 h and compared with the JCPDS data of CGO and $GdBaCo_2O_{5.54}$.

calculated TEC values from the plots, which exhibit the similar TEC of GBCO (20.0×10^{-6} °C^{-1}) compared with previous reports [9,12,16]. As expected, a further decrease in the TEC values was observed with the addition of CGO into GBCO. The TEC of GBCO decreased to 14.7×10^{-6} °C^{-1} for CG30 cathode. The reduction of the TEC of composite cathode is mainly attributed to the smaller TEC of CGO, for example, the TEC of CGO is 12×10^{-6} °C^{-1} [17]. Thus, the addition of CGO led to a decrease in the thermal expansion coefficient, which could give the thermal stability of the CG30 cathode [6].

Fig. 3 shows the impedance spectra of the symmetrical cells using different wt.% CG cathode at 650 °C. The resistivity ($R_p = R_1 + R_2$) was obtained by fitting the impedance spectrum with an equivalent circuit model (inset in Fig. 3). The intercepts of the semicircle on the real axis at high-frequency region represent the total ohmic resistivity (R_s) of the electrolyte, the current collectors and the lead wires. The impedance spectra consist of two depressed semicircle. This indicates that there are at least two electrode processes, corresponding to the two semicircles, during reduction of oxygen. The resistance at the high frequency is related with the

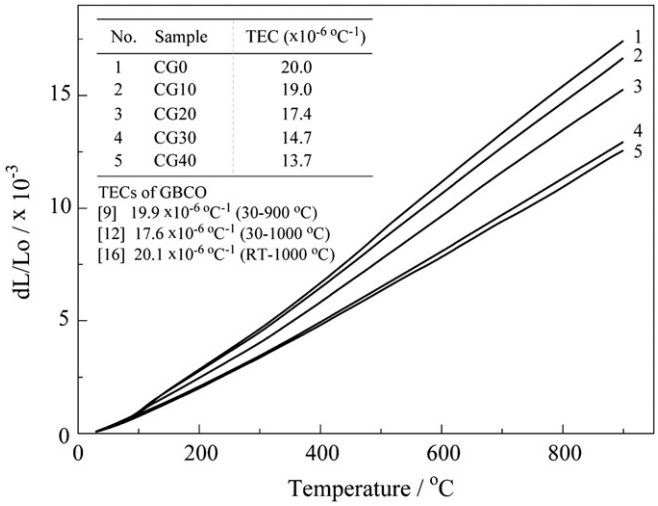

Fig. 2. Thermal expansion curves (dL/L_0) of CG composites in the temperature range of 30–900 °C in air. Inset Table shows the TEC values for CG composites.

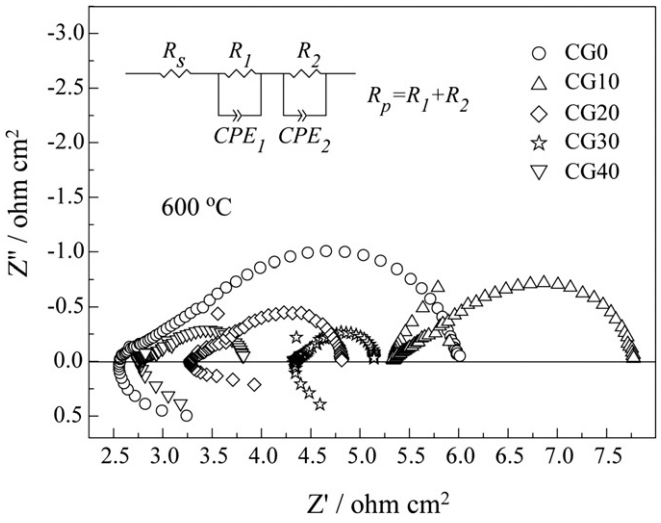

Fig. 3. Impedance spectra of the GBCO–CGO composite cathode measured at 600 °C.

charge-transfer process (R_1). The low-frequency arc can be attributed to the diffusion processes (R_2). The difference between real axes intercepts of the impedance plot is considered to be the electrode polarization resistance (R_p). CPE_1, CPE_2 correspond to the capacitance of the reaction related with the charge transfer and diffusion processes, respectively [2,5,14]. As shown in the Fig. 3, CGO content had a significant effect on the electrode polarization resistance of the cathodes.

The ARS values of the different wt.% CG composites from the interface resistances of the impedance spectra are shown in Fig. 4. The inset in Fig. 4 shows the ASR values as a function of the CGO content. Increasing the CGO content into the GBCO up to 30 wt.% resulted in a continuous decrease in polarization resistance at all temperatures. In Fig. 4, the CG30 composite cathode on the $Ce_{0.9}Gd_{0.1}O_{1.95}$ (CGO) electrolyte showed the lowest ASR value, where the values are about 0.029 and 0.012 Ω cm^2 at 700 and 750 °C, respectively, which is lower than the value of pristine GBCO cathode (0.194 and 0.082 Ω cm^2 at 700 and 750 °C, respectively). And the inset clearly exhibits that CG30 composite possesses the lowest ASR values. A further increase in CGO content to a value higher than 30 wt.% results in a higher interfacial polarization resistance. This may be due to a decrease in the electron-conducting path, which results in a decrease in the electrical conductivity [14,15].

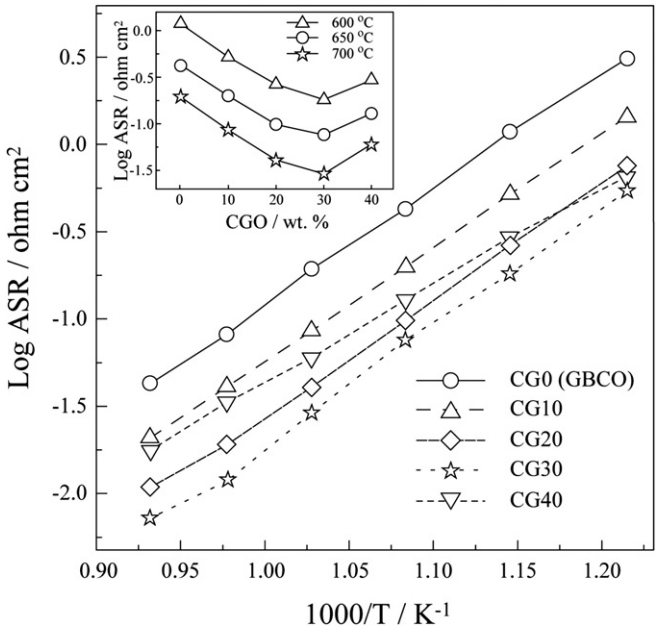

Fig. 4. Arrhenius plots of log ASR for the symmetrical cells of different wt.% CG/CGO at interface, measured in air. The insets show the ASR values *vs.* wt.% of composite electrodes.

It is widely accepted that addition of a highly conductive phase to the electrode, i.e, composite cathodes, is effective in expanding the electrochemically reaction zone from the limits of two-dimensional interface between the electrolyte and the cathode to the entire area of cathode [2,12–14]. As a result, addition of the high ionic conductive CGO in CG composite cathodes may provide additional electrochemically active area, i.e., the triple phase boundary where oxygen reduction reaction occurs. Improved performance of the composites cathode can be also explained by the increased oxygen conductivity [4]. Incorporation of the ionically conducting phase CGO, when added to a cathode, allowed CGO particle to connect GBCO grains, which provided the short-circuit paths for ion transport. This significantly improves the oxygen-ionic conductivity. Therefore, addition of CGO into the GBCO is effective in reduction of thermal expansion coefficient and improvement of the polarization resistance.

Fig. 5 shows the cross-sectional SEM image of the CG0 and CG30 cathode after the cell test. The SEM images of CG30 (Fig. 5 (b))

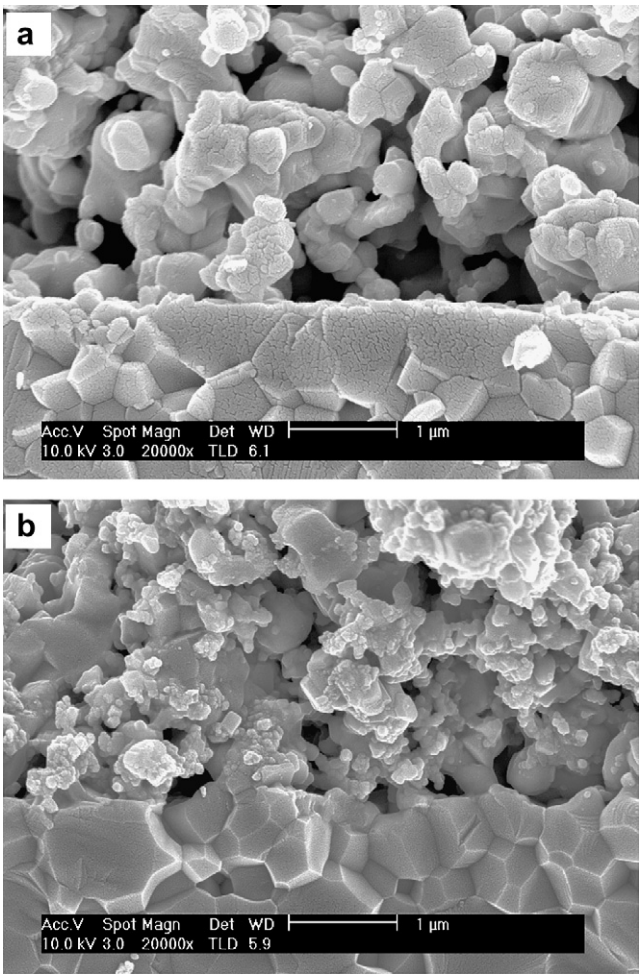

Fig. 5. SEM cross-sectional images of half-cells with (a) GGCO (CG0) and (b) CG30 composite cathode on CGO electrolyte after cell test.

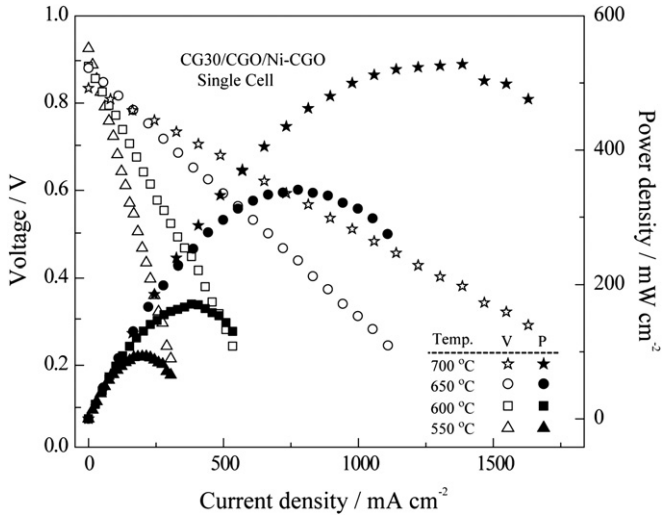

Fig. 6. Cell voltages (open symbols) and power densities (solid symbols) of CG30/CGO/Ni-CGO single-cells under humidified H_2 fuel and air oxidant at different temperatures.

expose a highly porous morphology that ensures good gas diffusion and presence of inter-connectivity at interfaces between the porous cathode and densified electrolyte. It is observed from Fig. 5 (b) that the CG30 composite cathode consists of homogenously distributed nano-size (~100 nm) spherical CGO particles on the surface of the bottleneck shaped GBCO particles (~1 μm). The CG30 cathode layer has a finer microstructure than the pure GBCO cathode (Fig. 5 (a)). The addition of CGO results in suppression of the growth of GBCO particles, and thus provides increased triple phase boundary [13,14]. In addition, homogeneous distribution of CGO in GBCO particle of CG30 composite may provide the short-circuit paths for ion transport and hence improves the oxygen-ionic conductivity [4] discussed in the previous sections. This typical morphology may be one of the reasons to reduce the cathode polarization during the oxygen reduction reaction. This supports the reason for enhancement of electrochemical performance of CG30 compared with pristine GBCO.

The cell voltage and the corresponding power density of electrolyte-supported single-cells configuration of CG30/CGO/Ni-CGO in the temperature 550–700 °C are shown in Fig. 6. The maximum power density of CG30 is 340, 525 mW cm^{-2} at 650 and 700 °C, respectively. These results demonstrate that CG30 cathode exhibits high performance compared with the data found in the literature of the pristine GBCO cathode [7,9–11]. Thus, it can be concluded that the enhanced electrochemical performance of CG30 cathode was attributed to the incorporation of the CGO to the GBCO. This has enlarged the triple phase boundary or simply provides short routes for ion transport for mixed conducting materials, which are advantageous for efficient oxygen reduction process and fast charge transport. Also, addition of CGO affected good inter-connectivity between the composite particles and interface of cathode and electrolyte due to the reduced TEC.

4. Conclusions

The GBCO–CGO composite cathodes were investigated for the potential cathode for IT-SOFCs. The different weight percentages of CG0 to CG40 composite cathodes were synthesized via the citrate combustion method followed by the precipitation method. The GBCO cathode revealed a good chemical compatibility with the CGO electrolyte. TEC values are reduced by mixing CGO and GBCO particles to form CG composite cathodes. This could improve the thermal stability of CG30 cathode by achieving a match of the TEC between electrolyte and cathode. The polarization resistance of the composites cathode has been measured by AC impedance spectroscopy. The impedance spectra results indicate that the incorporation of CGO to GBCO greatly improves electrochemical performance. Among the composites cathode, GBCO–30 wt.% CGO exhibits the highest cathode performance. The maximum power density of the electrolyte-supported single-cell CG30/CGO/Ni-CGO attained 340 and 525 mW cm^{-2} at 650 and 700 °C, respectively. These results indicate that CG30 is a promising cathode material for intermediate temperature SOFC cathode materials.

Acknowledgement

This work was financially supported by the Priority Research Centers Program through the National Research Foundation of Korea (NRF) (No. 2009-0094041), Center for ERC Program (2008-0062206) and by Brain Korea 21 (BK21) program funded by Korea government (MSET). D. S. Kim would like to thank the Korea Science and Engineering Foundation (KOSEF) funded by Korea government (MEST) (No. R01-2008-000-20480-0).

References

[1] V. Dusastre, J.A. Kilner, Solid State Ionics 126 (1999) 163.
[2] S.J. Lee, P. Muralidharan, S.H. Jo, D.K. Kim, Electrochem. Commun. 12 (2010) 808.
[3] Y. Liu, S. Hashimoto, K. Yasumoto, K. Takei, M. Mori, Y. Funahashi, Y. Fijishiro, A. Hirano, Y. Takeda, Curr. Appl. Phys. 9 (2009) S51.
[4] D. Chen, R. Ran, Z. Shao, J. Power Sources 195 (2010) 7187.
[5] W.-X. Kao, M.-C. Lee, T.-N. Lin, C.-H. Wang, Y.-C. Chang, J. Power Sources 195 (2010) 2220.
[6] K. Nagasawa, S. Daviero-Minaud, N. Preux, A. Rolle, P. Roussel, H. Nakatsugawa, O. Mentré, Chem. Mater. 21 (2009) 4738.
[7] J.-H. Kim, A. Manthiram, J. Electrochem. Soc. 155 (2008) B385.
[8] Q. Zhou, T. He, Y. Ji, J. Power Sources 185 (2008) 754.
[9] S.H. Jo, P. Muralidharan, D.K. Kim, Electrochem. Commun. 11 (2009) 2085.
[10] A. Tarancón, A. Morata, G. Dezanneau, S.J. Skinner, J.A. Kilner, S. Estradé, F. Hernández-Ramírez, F. Peiró, J.R. Morante, J. Power Sources 174 (2007) 255.
[11] J. Peña-Martínez, A. Tarancón, D. Marrero-López, J.C. Ruiz-Morales, P. Núñez, Fuel Cells 8 (2008) 351.
[12] Q. Zhou, F. Wang, Y. Shen, T. He, J. Power Sources 195 (2010) 2174.
[13] C. Zhu, X. Liu, D. Xu, D. Wang, D. Yan, L. Pei, T. Lü, W. Su, J. Power Sources 185 (2008) 212.
[14] H. Gu, H. Chen, L. Gao, L. Guo, Electrochim. Acta 54 (2009) 7094.
[15] Y.J. Leng, S.H. Chan, Q.L. Liu, Int. J. Hydrogen Energy 33 (2008) 3808.
[16] N. Li, Z. Lü, B. Wei, X. Huang, K. Chen, Y. Zhang, W. Su, J. Alloys Comp. 454 (2008) 274.
[17] G.A. Tompsett, N.M. Sammes, O. Yamamoto, J. Am. Ceram. Soc. 80 (1997) 3181.